ISTITUTO NAZIONALE DI FISICA NUCLEARE

Sezione di Genova

INFN/AE-86/12
28 Novembre 1986

C. Caso:

MEASUREMENTS OF D-MESON LIFETIMES IN NA27

Servizio Documentazione
dei Laboratori Nazionali di Frascati

INFN - Istituto Nazionale di Fisica Nucleare
Sezione di Genova

INFN/AE-86/12
28 Novembre 1986

MEASUREMENTS OF D-MESON LIFETIMES IN NA27‡

C. CASO

Dipartimento di Fisica and Sezione INFN, Genova, Italy.

1.- INTRODUCTION

Accurate measurements of heavy flavour lifetimes and branching ratios are the appropriate keys to have a coherent frame of charm and beauty weak decay. And over the last few years this field of physics has been very active from the experimental (as well as theoretical) side.

An updated summary of heavy flavour lifetimes can be found in [1] while for their production properties the interested reader is referred to [2] and [3].

In this talk I will cover the contributions given by the LEBC-EHS (experiment NA27) to the measurements of the D-meson lifetimes.

The menu of this talk will then be :

1) motivations for measuring charm lifetimes;
2) NA27 characteristics and charm strategy;
3) survey of four different methods used by this experiment to measure τ's ;
4) check and comparison of the results;
5) conclusions.

---

‡ Talk given at the EHS Symposium held at Balatonaliga (Hungary), 8-10 September 1986.

2.- MOTIVATIONS FOR MEASURING CHARM LIFETIMES

In this section I will only briefly mention the theoretical ideas which constitute the framework of our experimental results.

Figure 1(a) shows a sketch of a Cabibbo-favoured ($\Delta C = \Delta S = -1$) charmed meson decay. Similar diagrams can be drawn both for charm baryons and Cabibbo-forbidden decays . This diagram is the so called " spectator diagram " since only the charm quark undergoes a decay, while its partner light quark acts as a spectator.

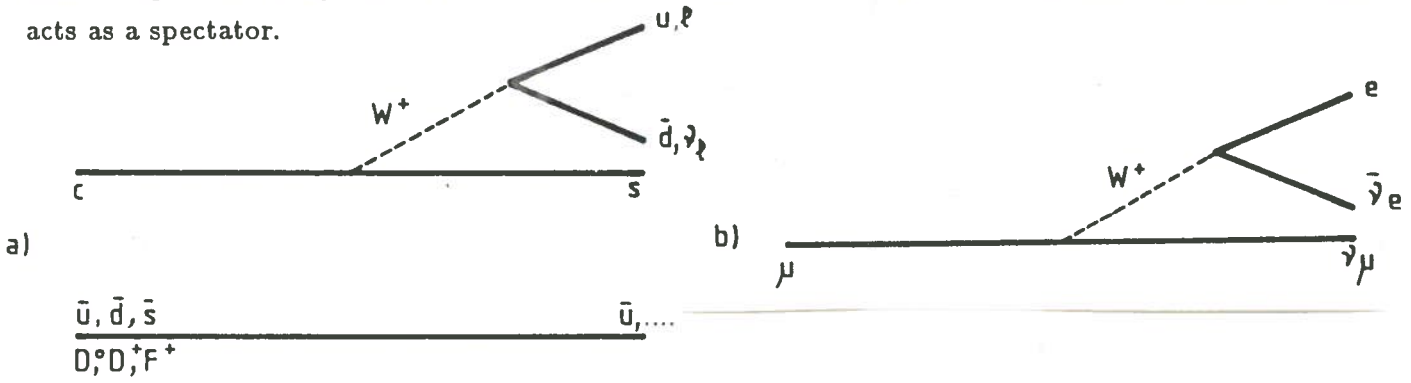

Fig. 1 Sketch of :
a) spectator diagram for a semileptonic and hadronic decay of a charmed meson ;
b) muon decay diagram.

Since the spectator diagrams are essentially the same for all charmed state decays, one could simply deduce that all charm particles must have the same lifetime .

This lifetime can be estimated comparing the spectator diagram to the muon decay diagram of fig. 1(b). This comparison predicts :

$$\tau(c) \approx 1/5\ (m_\mu/m_c)^5\ \tau(\mu) \qquad (1)$$

and then $\tau(c) \approx 3.5 \div 7.5\ 10^{-13}$ s depending on the mass of the c-quark.

Furthermore, since :

$$\tau \sim 1/\Gamma_{tot}\ , B_l = \Gamma_l\ (D \to l\nu X)/\Gamma_{tot}(D \to all) \qquad (2)$$

and

$$\Gamma_l\ (D^0 \to l\nu X) = \Gamma_l\ (D^\pm \to l\nu X) \qquad (3)$$

one can deduce that all charm particles must also have the same semileptonic branching ratio.

A naive numerical prediction of $B_l \approx 20\%$ is simply given by the three colours and two leptons in which the W of fig. 1(a) can decay. QCD corrections actually reduce the expected branching ratio for e-semileptonic decay to about 13%.

This simple scheme of a pure light quark spectator model is in strong disagreement with the MARK III experimental results [4] :

$$B_l\ (\mathrm{D}^0 \to l\nu\mathrm{X}) = (\ 7.5 \pm 1.1 \pm 0.4)\%$$
$$B_l\ (\mathrm{D}^\pm \to l\nu\mathrm{X}) = (17.0 \pm 1.9 \pm 0.7)\%$$
$$\mathrm{R} = B_l\ (\mathrm{D}^\pm \to l\nu\mathrm{X})\ /\ B_l\ (\mathrm{D}^0 \to l\nu\mathrm{X}) = 2.3\ ^{+0.5}_{-0.4} \pm 0.1$$

Note that so far nothing is known on D_S (formerly F) branching ratios.

Various mechanisms have been proposed to explain this inconsistency :

a) a destructive interference, due to the Fermi statistics, between the spectator antiquark $\bar{d}$ in the $D^{\pm}$ decay and the identical $\bar{d}$ from the non leptonic decay $c \rightarrow su\bar{d}$ (see fig. 2(a)). Since this interference will not occur in the D^0 decay, it would result in $\tau(D^{\pm}) > \tau(D^0)$. However, a detailed calculation [5] shows that this mechanism, although contributing in the right direction, can only play a marginal role ;

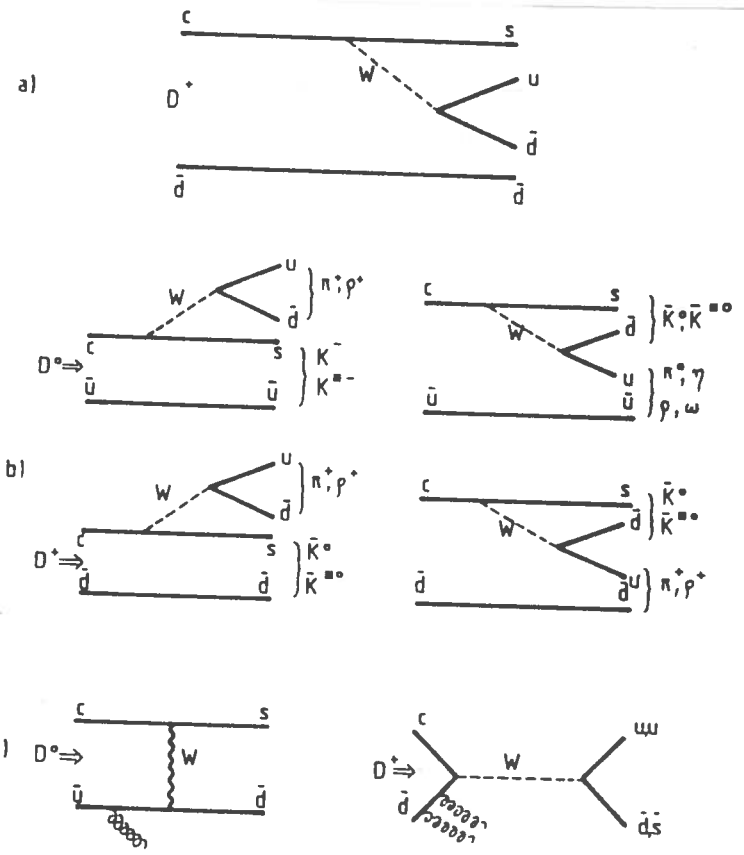

Fig. 2 Representation of :
a) internal spectator diagram for $D^{\pm}$ decay, showing the possible destructive interference due to the Fermi statistics ;
b) spectator diagrams (normal and internal) for both D^0 and $D^{\pm}$ decay . Final state hadrons are also reported ;
c) non-spectator diagrams for D^0 (W-exchange) and $D^{\pm}$ (annihilation) decay.

b) color-mixed spectator diagram. This possibility is diagrammatically indicated in fig. 2(b). The decay diagram reported on the right of each line is referred to as " internal spectator diagram". For the D^0 decay the normal and the internal spectator diagrams are incoherent since they lead to different final states, then no interference is possible. On the contrary, the $D^{\pm}$ decay diagrams lead to the same final states and they can then interfere. QCD shows that this interference is destructive, then giving $\tau(D^{\pm}) > \tau(D^0)$; however, QCD requires also colour suppression for the internal spectator diagram, and as a final result one has a non-significant interference ;

c) contribution of non-spectator diagrams. In the earlier calculations this contribution was disregarded, due to the helicity conservation which does not allow the coupling of the vector boson W to the pseudoscalar state $c\bar{q}$. However this suppression can be recovered taking into account emission of gluons by one of the initial quarks. Since in the non-spectator picture the $D^{\pm}$ annihilation is Cabibbo-suppressed (see fig 2(c)), the $D^{\pm}$ is expected to have a lifetime longer than that of the D^0, D_S and Λ_c.

The possibility for a non-spectator contribution seems to be confirmed by the experimental observation of the decay mode $D^0 \rightarrow \phi\overline{K}^0$ which is believed to occur uniquely via the W-exchange diagram.

ARGUS, MARK III and CLEO have all seen the decay $D^0 \to K^+K^-\overline{K}^0$ but for some time the branching ratio for $D^0 \to \phi\overline{K}^0$ has disagreed at the level of the interpretation of the background in the ϕ region.

There seems to be now a good agreement among the three groups (ARGUS : $1.18 \pm 0.25 \pm 0.17$; CLEO : $1.18 \pm 0.40 \pm 0.17$; MARK III : $1.1^{+0.7+0.4}_{-0.5-0.2}$ [6] to be compared with a rough expectation of $\approx 1.5\%$) whilst there is not yet a general consensus among theorists on the interpretation of this result, as it has been recently argued that the $D^0 \to \phi\overline{K}^0$ mode could also be generated via a multichannel final state interaction even if the W-exchange mechanism were absent [7].

It is clear from the above considerations that our present understanding of the charm decay dynamics is not satisfactory yet and then their lifetime measurements are needed and welcome.

3.- NA27 CHARACTERISTICS AND CHARM STRATEGY

I do not want to bother you here with a lot of details on the spectrometer, since all of you are also members of the EHS community ; the dedicated reader can anyway find all the relevant information in [8].

I want however to stress the unique features of the experiment NA27 :

1) the bubble chamber is filled with hydrogen, thus providing a negligible background of secondary interactions to charm decays ;

2) there is no charm trigger (only interaction trigger) so that there is no bias in data taking ;

3) the optical resolution is ≤ 20 μm, resulting in a very high scanning efficiency and two-track separation ;

4) the measurement precision achieved by the Strasbourg H.P.D. is illustrated by the following two numbers:

   ≈ 2.5 μm resolution on track impact parameter (see below for its definition) and ≈ 1.8 μm r.m.s. residual on HPD master points (≈ 30 points/track);

5) last but not least, a powerful particle identification.

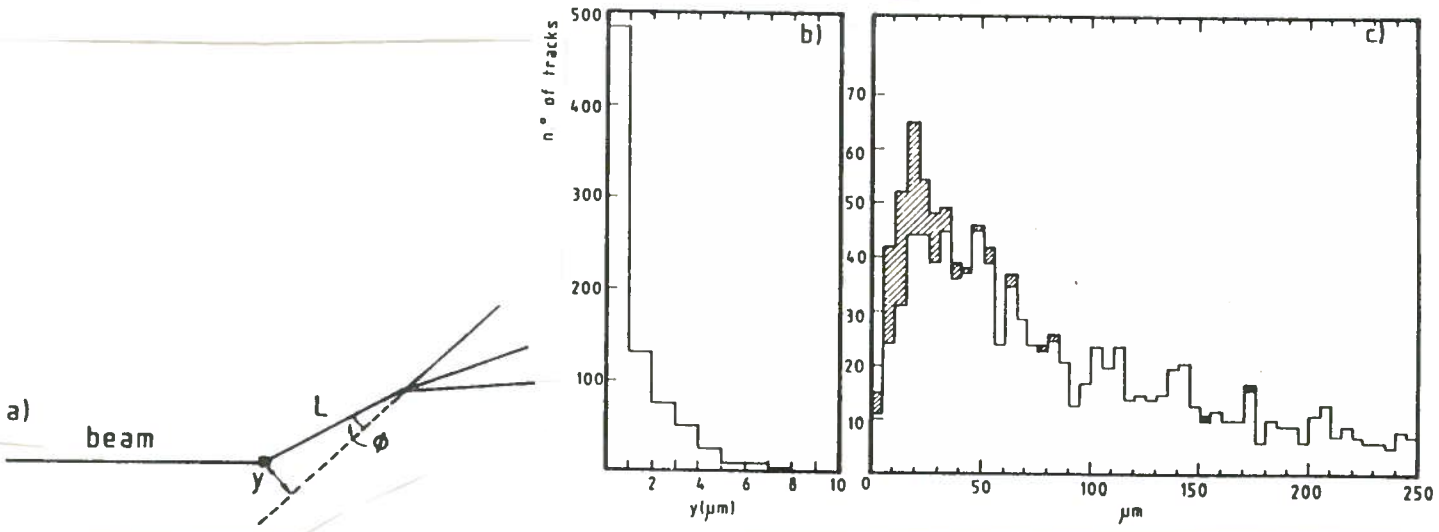

Fig. 3 a) definition of impact parameter $y = L \sin\phi$ for a track from a charged D decay ;
b) distribution of charged track impact parameters w.r.t. their vertex of origin ;
c) distribution of impact parameter of charged tracks from charm decay. The dashed part represents tracks added (or reassigned) during the HPD phase.

The basic experimental procedure to identify an interesting secondary activity is based upon the definition of the impact parameter y = L sinϕ given in fig. 3(a). Note that for LEBC y (film plane) $\approx$ y (space).

Since :

$$| L \sin\phi | = L\, p_T / p = p_T\, c\, t / m = O (c\, t) \qquad (4)$$

a scan inside a " charm-box " with a width of $\pm$ 2 mm transverse to the beam and extending through the whole bubble chamber has little effect on charm decays while strongly reduces the background of strange particles (since they have very different lifetimes).

Extensive tests have shown that :

a) scanning of secondary activities inside the charm-box has an efficiency of $\approx$ 100% if y$\geq$ 50 μm (which corresponds to about 2.5 bubble diameters);

b) the HPD precise measurement has a $\approx$ 100% efficiency down to y $\geq$ 7 μm ($\approx 3\sigma$ of the HPD measurement error).

All the above statements are proved by the histograms of fig. 3(b) and 3(c). Fig . 3(b) shows the distribution of the impact parameters for the main vertex and is a direct measurement of the impact parameter resolution (fig. 3(b) has $\sigma \approx$ 2.5 μm) . Fig. 3(c) shows the impact parameter distribution of tracks from charm decays; the dashed part of this histogram represents tracks that have been added (or reassigned when they were misassigned at the scanning) during the HPD measurement and clearly shows the capability of this device to clarify difficult topologies for 7 $\leq$ y $\leq$ 50 μm.

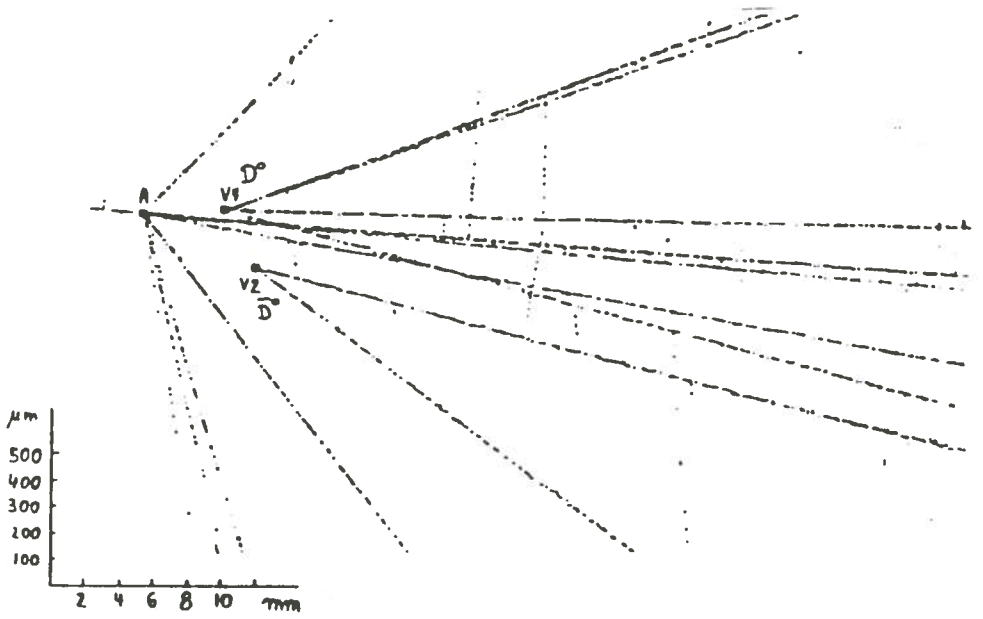

Fig. 4 An HPD digitization of a $D^0\overline{D^0}$ pair decaying respectively into four and two prongs. Note the different scales along and across the beam.

Fig. 4 shows an HPD digitization of a neutral D pair, decaying respectively into two and four prongs. To amplify the view of the decays, the digitizations are stretched across the beam.

To accept a decay for the lifetime study, an overall requirement of $y_{min} \geq 7$ μm and $y_{max} \geq 50$ μm is thus applied to ensure good visibility and detection.

Charged and neutral decays are classified as Cn and Vn respectively, where n is the number of charged decay products. Further requirements, depending on the topology, are applied to avoid any possible contamination :

1) C5 and V4 are straight accepted as charms ;

2) C3 are accepted as charms if paired with a second charm or if a decay track has $p_T \geq$ 250 MeV/c;

3) V2 are accepted as charms if paired with a second charm and if a decay track has $p_T \geq$ 250 MeV/c;

4) C1 are not used for lifetime but, if $p_T \geq$ 250 MeV/c, they can complete a charm pair.
In all above, p_T is calculated w.r.t the line of flight of the parent.

I want to stress here the severeness of these cuts. For the π^-p exposure, whose lifetime results I am going to present you, (360 GeV/c incident momentum, sensitivity of $\approx$ 15.8 events/μb) we have got 114 interactions containing 183 visible charm decays (45 single decays and 69 pairs). 100 are neutral and 83 are charged decays. The breakdown per topology is the following : 28 C1, 78 V2, 51 C3 (of which 3 Λ_c), 22 V4 and 4 C5. The above cuts reduce the D-lifetime sample to 93 decays (36 V2, 33 C3, 21 V4 and 3 C5) indicating that about 50% of the decays, although possessing a clear charm signature, do not enter the analysis.

4.- SURVEY OF DIFFERENT METHODS TO MEASURE LIFETIMES

For a given D decay, the proper flight time is given by $t = lm_D / cp_D$ where p_D and l are the charm momentum and length respectively. For an ideal experiment, with no losses, the lifetime would then be given by

$$\tau = \frac{\sum_{i=1}^{N} t_i}{N} \qquad (5)$$

where t_i are the individual proper times.

A way to correct for the real life losses occurring at very short and very long distances (losses due to both scanning and visibility inefficiencies and decays outside the fiducial volume) consists in giving a visibility weight which is a simple function of the minimum and maximum detectable length, l_{min} and l_{max}:

1) l_{min} is defined as the length necessary to detect, with efficiency close to 1, a track not originating from the primary vertex and it is obtained "swimming" the decay along its line of flight until y_{max} reduces to 50 μm or y_{min} reduces to 7 μm (l_{min} is the maximum of these two lengths);

2) l_{max} is computed taking into account the finite length of LEBC, the optical depth of focus ($\pm$2 mm) and the boundaries of the charm box.

After this general introduction that defines quantities used in all methods, I would like to go through the different techniques used by NA27 to extract lifetimes.These methods are :

1) constrained kinematical fits;
2) momentum estimator;
4) impact parameter;
4) transverse length.

Due to lack of time, I will only try to touch the most peculiar features of each method, without fully entering into the technicalities ; a complete account of the details is given in [9].

4.1.- constrained kinematical fits

There is very little to say about this method, since it is classic and certainly superior in principle since there is no model dependency in it. However it in no way makes full use of the available data sample, because of the need for a well determined momentum.

Performing a maximum likelihood fit of the type :

$$\mathcal{L}(\tau) = \prod_i \frac{1}{\tau} \frac{\exp(-t^i/\tau)}{\exp(-t^i_{min}/\tau) - \exp(-t^i_{max}/\tau)} \tag{6}$$

we find the following lifetime values :

$$\tau(D^{\pm}) = (9.8^{+3.4}_{-2.2})10^{-13}\ s \quad (20\ C3/C5\ decays)$$

$$\tau(D^0) = (3.6^{+1.0}_{-0.7})10^{-13}\ s \quad (21\ V2/V4\ decays)$$

giving a ratio $R = \tau(D^{\pm})/\tau(D^0) = 2.7^{+1.2}_{-0.8}$.

Here and in all what follows the errors quoted correspond to a fall in the log likelihood from the maximum by 0.5. Furthermore in this section I will give D^0 lifetimes as obtained combining the V2 and V4 sample. Possible differences between the two samples will be discussed in Sect. 5.

4.2.- momentum estimator

This technique, originally proposed by Franek [10], has been extended to allow more general applications; details of this extension can be found in [11]. The estimator method is based on the following general philosophy : since τ is the average of t^i (or of $t^i - t^i_{min}$ in the case of a negligible l_{max} effect) one does not really need to know the individual charm momenta p^i_D precisely, but to be correct on the average. This point of view implies that also unconstrained decays may be included in the lifetime calculation, provided that an unbiased scaling law to "estimate" its momentum is found.

To derive this "magic formula" let first Lorentz transform between the lab and the D rest frame :

$$p_{vis} = \gamma\,(p^*_{vis}\,cos\theta + \beta E^*_{vis}) \tag{7}$$

where γ and β are the usual boost parameters and θ is the angle between $\vec{\beta}$ and $\vec{p}^*_{vis}$ (in D-rest frame). Taking the average (keeping p_D and m_{vis} fixed):

$$< p_{vis} > = E_D/m_D < p^*_{vis}\,cos\theta > + p_D/m_D < E^*_{vis} > \tag{8}$$

Since the D-meson is unpolarized and the spectrometer has $\approx$ 100% acceptance in the forward region ($x_F > 0$, where we apply the estimator method) $< p^*_{vis}\,cos\theta > = 0$. Furthermore :

$$E^*_{vis} = (p^{*2}_{vis} + m^{*2}_{vis})^{1/2} = m_{vis}\,(1 + p^{*2}_{vis}/m^{*2}_{vis})^{1/2} = \beta\, m_{vis} \tag{9}$$

with β close to 1 since for a D decay $|\vec{p}^*_{vis}| \ll m_{vis}$. Then :

$$< p_{vis} > = (p_D/m_D)\beta\, m_{vis} \tag{10}$$

If we now define : $p^{est}_D = m_D\, p_{vis}/\beta\, m_{vis}$ we have that p^{est}_D is an unbiased estimate of p_D since :

$$< p^{est}_D > = m_D < p_{vis} > /m_{vis}\,\beta = p_D \tag{11}$$

As charged particles are not always fully identified, $m_{vis} = \delta\, m^{\pi}_{vis}$, with all charged particles assumed to be pions ($\delta \approx 1$) . So one finally gets the "magic formula" :

$$p_D^{est} = \alpha\, m_D\, p_{vis} / m^{\pi}_{vis} \quad with\ \beta\delta = \alpha^{-1} \tag{12}$$

The dependence of α on m^{π}_{vis} and p_{vis} has been determined by Montecarlo. Fig. 5(a) shows the distribution of α for D^0 (both V2 and V4) as a function of m^{π}_{vis} averaged over p_{vis} while fig. 5(b) shows the same dependence for α^{-1} (note that α gives p^{est} and then $(x_F)^{est}$, while α^{-1} gives t^{est}). The broad distribution in α and α^{-1} at small values of m^{π}_{vis} corresponds to a poor determination of the lifetime when a lot of momentum is not measured by the spectrometer ; the distribution becomes narrower as m^{π}_{vis} (and p_{vis}) increases.

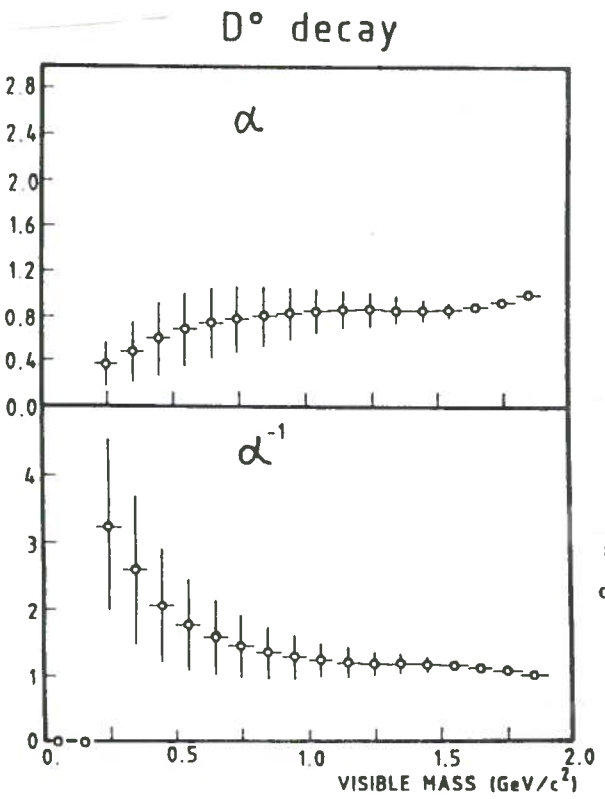

Fig. 5

a) Montecarlo results for the estimator analysis showing the dependence of α on m^{π}_{vis} (integrated over p_{vis}) for a D^0 decay;

b) the same Montecarlo dependence for α^{-1}.

To show that the method works well, we present in fig. 6 some Montecarlo results obtained generating 500 experiments each consisting of 50 D^0 decays. The distribution of the true mean lifetimes is plotted in fig. 6(a) while the corresponding D^0 lifetimes predicted by the estimator analysis are reported in fig. 6(b). Both distributions are well centered around 1, as expected ; the estimated lifetime distribution has an r.m.s. of 0.180, to be compared with an r.m.s. of 0.148 of the true life distribution.

For the lifetime determination, rather than using the average value of α that corresponds to the particular combination of p_{vis} and m^{π}_{vis} to obtain a unique value of p^{est} for each decay, the distribution of p^{est} as given by $dN/d\alpha$ is used. Since :

$$\frac{\partial^2 N}{\partial l\, \partial \alpha} = \frac{1}{\lambda(\alpha)} \exp[-l/\lambda(\alpha)]\, f(\alpha) \tag{13}$$

where :

$$f(\alpha) = \frac{dN}{d\alpha} \quad , \quad \lambda(\alpha) = \alpha\, \frac{p_{vis} c\tau}{m^{\pi}_{vis}} \tag{14}$$

the normalized likelihood function is :

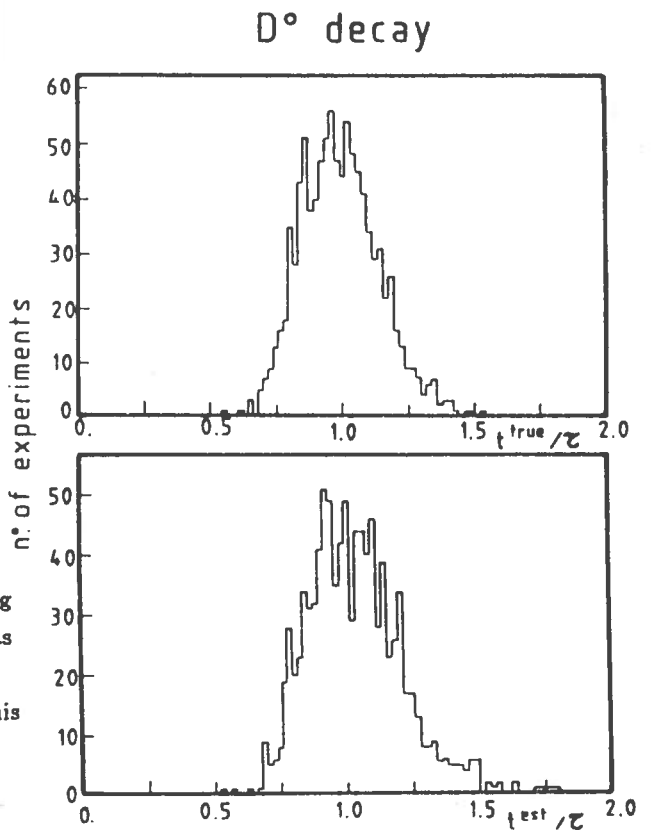

Fig. 6 a) Montecarlo results for the estimator analysis showing the distribution of t^{true}/τ for D^0 decays. This distribution has a mean value of 0.997 and an r.m.s. of 0.148 ;
b) similar Montecarlo distribution for t^{est}/τ for D^0 decays. This distribution has a mean value of 1.036 and an r.m.s. of 0.180.

$$\mathcal{L}(\tau) = \prod_i \frac{\int_0^\infty \frac{1}{\lambda^i(\alpha)} \exp[-l^i/\lambda^i(\alpha)]\, f^i(\alpha) d\alpha}{\int_0^\infty \{\exp[-\frac{l^i_{min}}{\lambda^i(\alpha)}] - \exp[-\frac{l^i_{max}}{\lambda^i(\alpha)}]\} f^i(\alpha) d\alpha} \qquad (15)$$

where the integrations are performed numerically.

The lifetimes obtained using the estimator analysis are :

$$\tau(D^\pm) = (11.5^{+4.5}_{-2.8})10^{-13}\ s \quad (20\ C3/C5\ decays)$$

$$\tau(D^0) = (4.4^{+1.0}_{-0.7})10^{-13}\ s \quad (36\ V2/V4\ decays)$$

with a ratio $R = \tau(D^\pm)/\tau(D^0) = 2.6^{+1.2}_{-0.8}$.

Note that since this method requires a certain degree of knowledge on the momentum of the decay, we have applied cuts in addition to those used to define the full sample. We have required that : (a) at least two tracks are hybridized in the spectrometer ; (b) $(x_F)^{est} > 0$.

4.3.- impact parameter

This technique has been extensively used by many other experiments and it is based upon the fact that, as already mentioned in Sect. 3, for a particular decay track the impact parameter is of the order of ct, where t is the charm proper time. Then, in absence of cuts on the data,the average impact parameter will

result to be proportional to the lifetime τ. Details on this method can be found in [12] and [13].

To determine the "calibration curve",i.e. the dependence of <y> on τ, we have used a Montecarlo which has different lifetimes as input, both for charged and neutral decays.

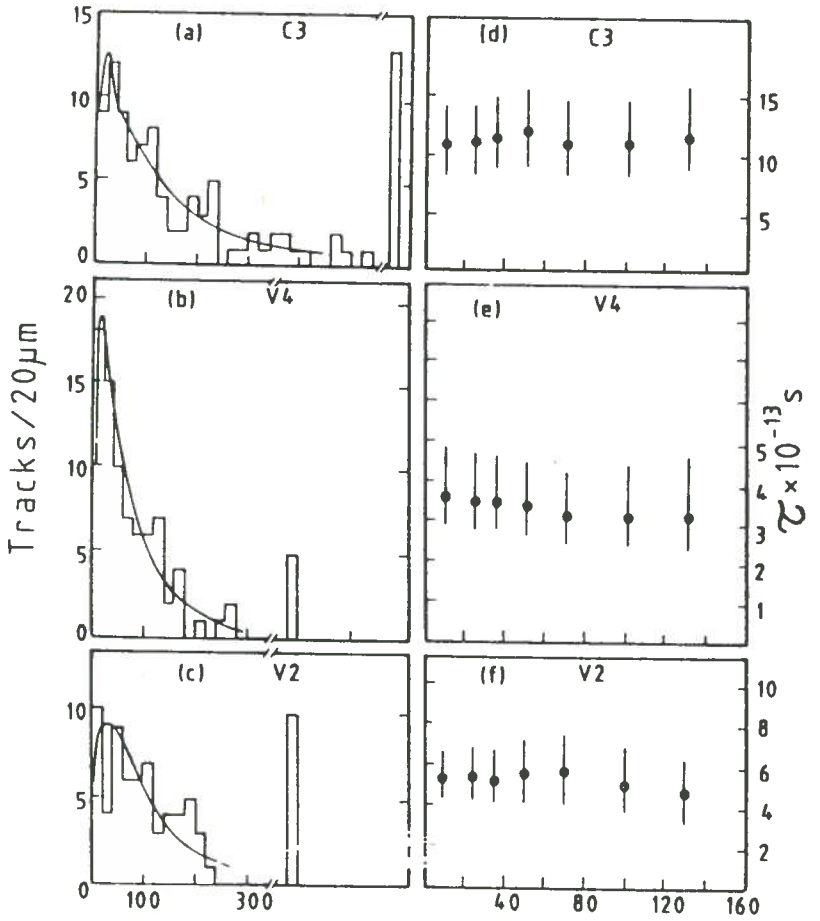

Fig. 7 Distributions of measured impact parameters. The curves in (a), (b) and (c) are the expected distributions for the lifetimes derived from the mean y and quoted in the text . In (d),(e) and (f) the lifetime results are plotted as a function of the y_{max} cut.

Fig. 7 shows the distributions of the measured impact parameters, together with the curves corresponding to the appropriate lifetimes given below. From fig. 7(a) and 7(b) one observes that the experimental impact parameter distributions are very well reproduced by their respective Montecarlo predictions; in fig. 7(c) there is an excess of large impacts which raises the mean impact parameter for the V2 topology. This excess is due to a V2 charm decay whose statistical significance in terms of anomalously living decay will be discussed in Sect. 5.

Fig. 7(d),(e) and (f) contain the dependence of the lifetimes on the maximum impact parameter cut, y_{max}. The results appear stable, indicating that they are not too sensitive to the precise value of the cut. Furthermore, for C3 topology, we do not observe any significant Λ_c and/or F contamination that would affect the region of low y_{max}.

The lifetimes we find using this method are :

$$\tau(D^{\pm}) = (11.9^{+3.9}_{-2.6})10^{-13}\ s \quad (33\ C3\ decays)$$

$$\tau(D^{0}) = (4.6^{+1.0}_{-0.7})10^{-13}\ s \quad (57\ V2/V4\ decays)$$

with a ratio $R = \tau(D^{\pm})/\tau(D^{0}) = 2.6^{+1.0}_{-0.7}$.

4.4.- transverse length

This method has been developed inside our collaboration and a full description of it can be found in [14]. The interest of this new technique is in the fact that it allows to use the full statistics available for the lifetime analysis and that it is model independent. It simply uses the correlation that exists between the transverse decay length l_T and the lifetime :

$$l_T = t p_T c/m \tag{16}$$

Since p_T and t are independent :

$$\frac{\partial^2 N}{\partial p_T \partial t} = \frac{1}{\tau} \exp[-t/\tau]\ F(p_T) \tag{17}$$

where $F(p_T)$ represents the functional form of the p_T distribution. Transforming variables from p_T and t to p_T and l_T one obtains :

$$\frac{\partial^2 N}{\partial l_T \partial p_T} = \frac{m}{p_T c\tau} \exp[-m l_T/p_T c\tau]\ F(p_T) \tag{18}$$

and then :

$$\frac{d\,N}{d\,l_T} = \int_0^\infty \frac{m}{p_T c\tau} \exp[-m l_T/p_T c\tau]\ F(p_T) dp_T \tag{19}$$

The p_T^2-dependence of the cross section has been measured [15] to be of the form $\exp(-\alpha p_T^2)$ with $\alpha = < p_T^2 >^{-1} = 1.18^{+0.18}_{-0.16}\ (GeV/c)^{-2}$. Note that α turns out to be the same both for D^0 and for $D^\pm$.

The transverse length method has to face a serious problem when trying to write a properly normalized likelihood function. Since there are cuts to apply to the data to ensure a high detection efficiency, one has to project the l^i_{min} and l^i_{max} discussed above into their projections l^i_{Tmin} and l^i_{Tmax} in the plane transverse to the beam. However this projection can only be made if the production angle θ^i is fixed, which is not the case since the longitudinal momentum cannot vary independently of the transverse momentum. Neglecting the kinematic constraints needed to keep θ^i fixed , the likelihood function can be approximated as :

$$\mathcal{L}(\tau) = \prod_i \int_0^\infty \frac{m}{p_T c\tau} \frac{\exp[-l^i_T m/p_T c\tau]}{\{\exp[-\frac{l^i_{Tmin} m}{p_T c\tau}] - \exp[-\frac{l^i_{Tmax} m}{p_T c\tau}]\}} F(p_T) dp_T \tag{20}$$

The amount of approximation introduced neglecting the complex but rigorous normalization has been studied by Montecarlo and the resulting correction factor is plotted in fig. 8 as a function of the input lifetime. It is seen that the above approximated likelihood function gives a slight overestimate of the lifetime.

Taking into account this correction factor, the lifetime values are :

$$\tau(D^\pm) = (10.4^{+2.8}_{-2.0}) 10^{-13}\ s \quad (36\ C3/C5\ decays)$$

$$\tau(D^0) = (4.5^{+0.8}_{-0.7}) 10^{-13}\ s \quad (57\ V2/V4\ decays)$$

with a ratio $R = \tau(D^\pm)/\tau(D^0) = 2.3^{+1.0}_{-0.7}$.

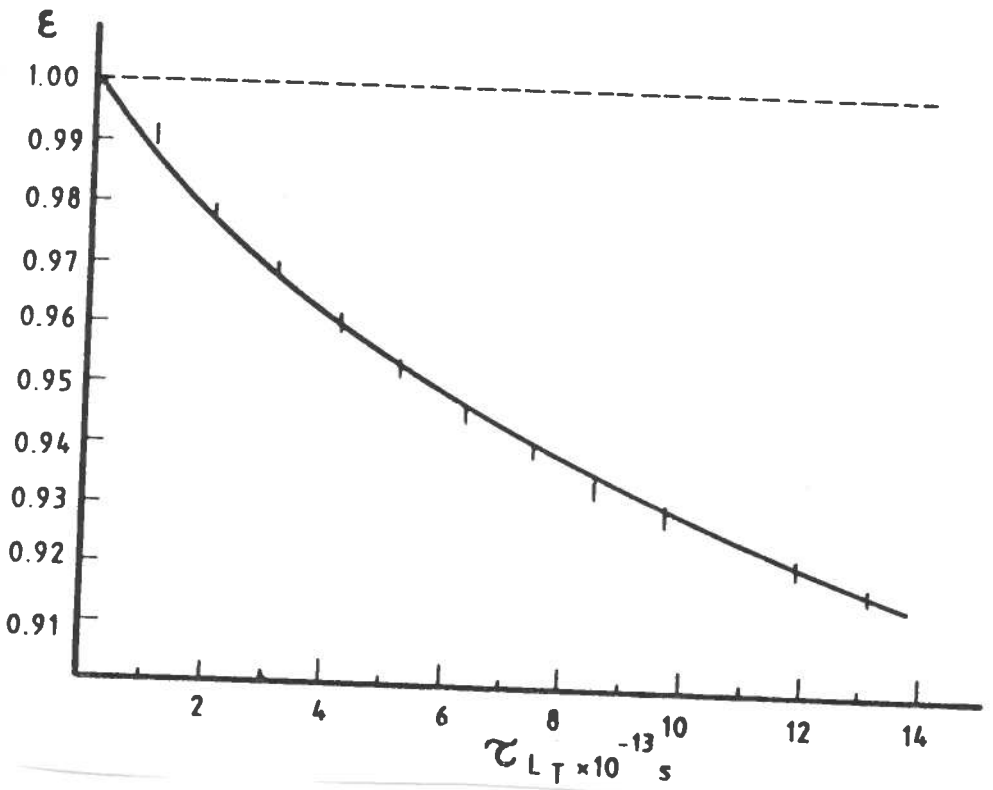

Fig. 8 Correction factor applied to the results of the transverse length analysis as a function of the lifetime.

In this case the errors include a systematic error (which does not affect the ratio R) due to the uncertainty in the slope α of the p_T^2 differential cross section. To get a feeling of the size of this contribution, a $\approx$ 10% systematic error in α propagates into a $\approx$ 5% change in lifetime.

Fig. 9 shows the distributions of $l_T - l_{Tmin}$ for both neutral and charged D. The curves correspond to the above lifetimes. From the mean values of these two distributions (57 μm for D^0 , 130 μm for $D^{\pm}$) one sees immediately that the lifetime ratio is $\approx$ 2.3.

The transverse length technique has the advantage that it can be directly checked against any subsample. Applying this analysis to the same events with a kinematic fit presented in Sect. 4.1, we obtain the following set of results (all lifetimes are $\times$ 10^{-13} s) :

D^0(V2)	D^0(V4)	D^0(V2+V4)	$D^{\pm}$
10 decays	11 decays	21 decays	20 decays
$3.6^{+1.5}_{-1.0}$	$3.5^{+1.4}_{-0.9}$	$3.6^{+1.0}_{-0.7}$	$9.8^{+3.4}_{-2.2}$
$4.3^{+2.1}_{-1.3}$	$3.2^{+1.6}_{-1.0}$	$3.6^{+1.3}_{-0.8}$	$9.8^{+3.7}_{-2.5}$

Here , for sake of completeness, I have split the D^0 results into V2 and V4. The first line of the table contains the lifetimes for the events with a kinematic fit , while the second line refers to the transverse length method applied to the same events. It is evident that this technique, when applied to the same event sample, returns very consistent results, giving confidence in the method.

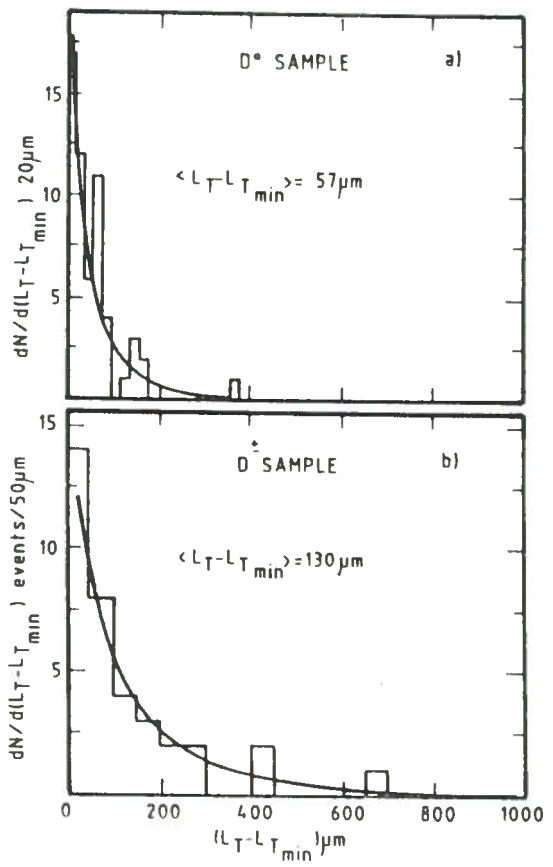

Fig. 9 Transverse length distributions for neutral and charged D. l_{Tmin} represents the minimum detectable transverse length for the particular event. The curves are the fits corresponding to the lifetimes given in the text.

5.- CHECK AND COMPARISON OF THE RESULTS

The results obtained in the previous section are all collected in the following table (all lifetimes are again $\times\ 10^{-13}$ s) :

	D^0(V2)	D^0(V4)	D^0(V2+V4)	$D^\pm$	R
Kin. fits	$3.6^{+1.5}_{-1.0}$	$3.5^{+1.4}_{-0.9}$	$3.6^{+1.0}_{-0.7}$	$9.8^{+3.4}_{-2.2}$	$2.7^{+1.2}_{-0.8}$
l_T	$4.8^{+1.1}_{-1.0}$	$3.8^{+1.3}_{-0.9}$	$4.5^{+0.8}_{-0.7}$	$10.4^{+2.8}_{-2.0}$	$2.3^{+1.0}_{-0.7}$
Estimator	$4.8^{+1.4}_{-1.0}$	$3.7^{+1.5}_{-0.9}$	$4.4^{+1.0}_{-0.7}$	$11.5^{+4.5}_{-2.8}$	$2.6^{+1.2}_{-0.8}$
Imp. par.	$5.6^{+1.7}_{-1.2}$	$3.4^{+1.2}_{-0.7}$	$4.6^{+1.0}_{-0.7}$	$11.9^{+3.9}_{-2.6}$	$2.6^{+1.0}_{-0.7}$

An overall comparison shows that :

a) all the indirect techniques give very consistent results;

b) the indirect techniques applied to the V2 decays all yield a larger $\tau(D^0)$ than the V4 decays. One decay contributes significantly to the indirect V2 result. This decay does not have a kinematic fit but possible 0C solutions indicate a lifetime in the range 17-30 10^{-13} s. If it is omitted from the V2 sample, the transverse length result is unaffected, since its l_T does not appear to be anomalous. However, the estimator result reduces to $(4.1^{+1.1}_{-0.8})\ 10^{-13}$ s for the V2 decays and the impact parameter result to $(5.1^{+1.6}_{-1.0})\ 10^{-13}$ s. The indirect technique results for the V2 sample remain consistent; however they are still higher than the V4 results. For a D^0 lifetime of 4.1 10^{-13} s, we would expect 0.6 events in our sample with t> 20 10^{-13} s. This event is therefore consistent with a D^0 lifetime of 4.1 10^{-13} s.

Since the transverse length method is model independent and makes full use of the unfitted decays, we give our final results as a combination of the kinematic fits, when available, and the transverse length applied to the remaining no fits. We then quote :

$$\tau(D^{\pm}) = (10.7^{+2.8}_{-1.8})10^{-13}\ s \quad (40\ C3/C5\ decays)$$

$$\tau(D^{0}) = (4.1^{+0.7}_{-0.6})10^{-13}\ s \quad (60\ V2/V4\ decays)$$

with a ratio $R = \tau(D^{\pm})/\tau(D^{0}) = 2.6^{+0.8}_{-0.6}$.

For those of you who are not really in the business of lifetimes, I have prepared a summary of charm lifetimes from around the world. Recent and less recent results are compiled in fig. 10 for $\tau(D^0)$ and in fig. 11 for $\tau(D^{\pm})$. To appreciate our results, I have compared them with the "world averages" and the reader can judge by himself the level of agreement.

I want to stress that the results covered by this talk refer only to the π^--proton exposure that has a sensitivity of (15.8±0.8) events/μb. This is only about a third of the full statistics available to NA27 which includes also a 400 GeV/c proton-proton exposure. Final lifetime values using the whole statistics will appear soon.

6.- CONCLUSIONS

Since it is now the good time to come to an end, I would like to conclude this talk with the following points :

a) a coherent frame of charm (and beauty) decay has not yet emerged, but it will do (hopefully) soon. Accurate measurements of lifetimes and branching ratios are an essential ingredient;

b) NA27 can give (and has already given) an important contribution to this puzzle. Four methods for lifetime determination have been studied, three of which do not depend on the kinematic fit. All these methods give stable and consistent results. Best values for $\tau(D^0)$ and $\tau(D^{\pm})$ are obtained using fits, when available, and the transverse length technique applied to the remaining no fits. Our best lifetime values are :

$$\tau(D^{\pm}) = (10.7^{+2.8}_{-1.8})10^{-13}\ s \quad (40\ C3/C5\ decays)$$

$$\tau(D^{0}) = (4.1^{+0.7}_{-0.6})10^{-13}\ s \quad (60\ V2/V4\ decays)$$

corresponding to a ratio $R = \tau(D^{\pm})/\tau(D^{0}) = 2.6^{+0.8}_{-0.6}$;

c) in the near future, NA27 will update the previous results using as thrice as much statistics.

7.- ACKNOWLEDGEMENTS

I wish to thank the Organizing Committee for the warm hospitality and for the perfect organization of this Symposium.

Thank are due to all my colleagues of the NA27 Collaboration ; in particular I am indebted for useful and illuminating discussions with G. Borreani, P. Checchia, C. Defoix, C. Fisher, D. Gibaut, J. Fry, S. Hellman, L. Montanet, G.D. Patel and K. Roberts.

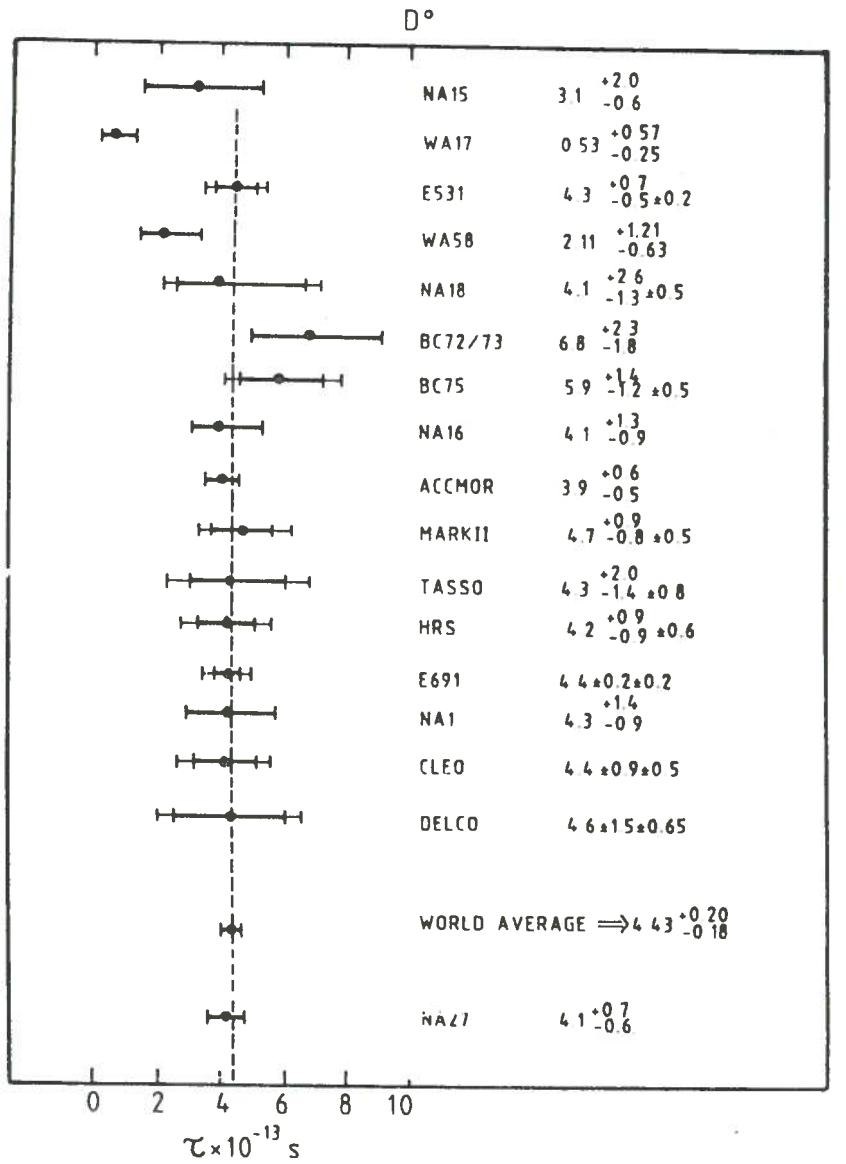

Fig. 10 Compilation of D^0 lifetimes.

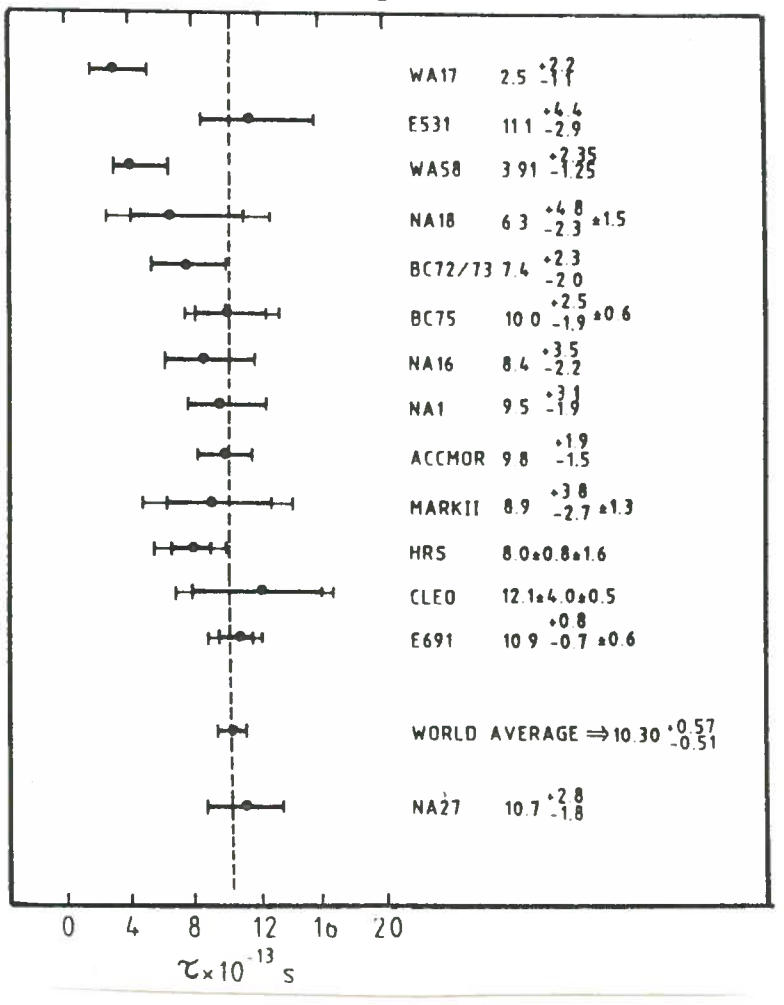

Fig. 11 Compilation of $D^{\pm}$ lifetimes.

References

[1] C. Caso and M.C. Touboul, Measurements of Heavy Flavour Lifetimes, CERN/EP 85-176. See also the addendum INFN GE/AE 86-10.

[2] C. Caso, Proceedings of the 1985 Kyoto International Symposium on Lepton and Photon Interactions, Kyoto, August 19-24, 1985, Eds. M. Konuma and K. Takahashi, pag. 488.

[3] A. Kernan and G. VanDalen, Phys. Rep. 106 (1984) 297.

[4] D. Hauser, MARK III Collaboration, XXth Rencontre de Moriond, 1985.

[5] G. Altarelli and M. Maiani, Phys. Lett. 118B (1982) 414.

[6] M.G.D. Gilchriese, CP violation and Weak Interactions of Light and Heavy Leptons and Quarks, Rapporteur talk at the XXIII International Conference on High Energy Physics, Berkeley, California, July 16-23, 1986.

[7] J.F. Donoghue, Phys. Rev D33, (1986) 1516.

[8] M. Aguilar-Benitez, LEBC-EHS Collaboration, Z. Phys. C, Particles and Fields 31 (1986) 491.

[9] M. Aguilar-Benitez, LEBC-EHS Collaboration, CERN EP 86-167, submitted to Z. Phys. C, Particles and Fields.

[10] B. Franek, Rutherford Report RAL 85-026 (1985).

[11] D. Gibaut, PhD. Thesis, University of Oxford (1986).

[12] S.Petrera and G. Romano, Nucl. Instr. and Meth. 174 (1980) 61.

[13] P. Checchia et al., INFN Note INFN/PD/EHS 84.

[14] K. Roberts, PhD. Thesis, University of Liverpool (1986).

[15] M. Aguilar-Benitez et al., LEBC-EHS Collaboration, Phys. Lett. 161B, 4 (1985) 400.